Journal of Clinical & Experimental Cardiology

Naum et al. J Clinic Experiment Cardiol 2011, S:5
DOI: 10.4172/2155-9880.S5-002

Research Article Open Access

Quantitative Comparison of Myocardial Perfusion Defects using Different Reconstruction Algorithms

Alexandru Naum[1], Nina Kleven-Madsen[1], Martin Biermann[1,2], Boel Johnsen[1], Birger A Tvedt[1], Svein Rotevatn[3], Jan Erik Nordrehaug[3,4] and Tore Bach-Gansmo[5]*

[1]*Centre for Nuclear Medicine/PET, Department of Radiology, Haukeland University Hospital, Bergen, Norway*
[2]*Section for Radiology, Institute for Surgical Sciences, University of Bergen, Norway*
[3]*Department of Heart Disease, Haukeland University Hospital, Bergen, Norway*
[4]*Institute of Medicine, University of Bergen, Norway*
[5]*Department of Radiology and Nuclear Medicine, Oslo University Hospital Ullevål, Oslo, Norway*

Abstract

Objective: To investigate the impact of a reconstruction method incorporating corrections for scatter, attenuation, and distance dependent detector response on cardiac single emission computed tomography (SPECT) perfusion studies compared with filtered back projection (FBP).

Materials and methods: A total of 20 patients underwent same-day, rest-stress SPECT/CT myocardial perfusion imaging. Images were reconstructed using iterative 3D ordered-subsets expectation-maximization (OSEM 3D) and FBP algorithms. Stress and rest myocardial perfusion defects were quantified using polar maps and normal database comparisons. The Bland-Altman plots were used to assess their degree of agreement. Results were confirmed by coronary angiography. The contrast, contrast to noise ratio and signal to noise ratio were used for the quantitative evaluation of the reconstruction quality.

Results: Perfusion defect extent quantification on OSEM 3D reconstructed images agreed and correlated well with defect extent quantification on FBP reconstructed images (bias ± standard deviation, -15% ± 20; r = 0.63) during stress and at rest (-10% ±15; r=0.70). Agreement and correlation were similar for severity scores during stress (-1.02 ± 1.77 SD's; r=0.62), and at rest (-1.10 ± 1.49 SD's; r=0.61). There were no statistically significant differences between the methods regarding perfusion defect extent or severity. The overall agreement rate with coronary angiography was similar. OSEM 3D reconstruction algorithm significantly increases the image contrast by 31% (P<0.05).

Conclusions: Compensation for detector response, attenuation and scatter improves image contrast compared with FBP. Applying quantitative analysis, OSEM 3D reconstruction produced increased image contrast compared to FBP, but similar results regarding the size and severity of left ventricular perfusion defects.

Keywords: Myocardial perfusion; Cardiac SPECT; OSEM 3D reconstruction; FBP reconstruction; Coronary angiography

Introduction

Myocardial perfusion imaging (MPI) using single-photon emission tomography (SPECT) is a widely used noninvasive modality in the diagnosis of coronary artery disease (CAD) and for assessing the functional significance of coronary stenoses [1,2]. An adequate image reconstruction algorithm is essential for image quality and diagnostic value of the technique. The routine for cardiac SPECT image reconstruction that has been used for many years was filtered back-projection (FBP) [3]. It is computationally fast, easy to implement, and widely clinically applied. Nevertheless, the FBP reconstructed images are degraded by a number of factors including soft tissue attenuation, Compton scatter, and collimator blurring, which limit spatial resolution, degrade the image contrast, and may distort the shape of left ventricular (LV) myocardium [4]. The introduction of hybrid SPECT/CT scanners in nuclear cardiology offers the potential of performing CT-based attenuation correction (AC) of the emissions scans, thus optimizing the diagnostic capabilities of cardiac SPECT. New reconstruction algorithms have been developed to include attenuation correction in the reconstruction process, as well as other parameters, such as depth-dependent collimator blurring and scatter [5-7]. Recent work has indicated that iterative reconstruction (IR) algorithms can be used to model the spatial resolution and sensitivity and compensate for the effects of scatter and attenuation when using CT [8-10]. Currently, ordered-subset expectation maximization (OSEM) is the preferred iterative method for reconstructing cardiac SPECT studies. Published data have demonstrated the ability of OSEM to improve lesion detectability, overall image quality and contrast, indicating a substantial advantage over the conventional FBP method [11,12]. This is particularly important for the interpretation of image data affected by visceral activity, breast tissue attenuation in women, or diaphragmatic attenuation, which can be confused with true perfusion defects.

The current study seeks to evaluate the overall cardiac image quality of the OSEM with three dimensional resolution recovery (OSEM 3D) and CT based attenuation correction as compared to the conventional FBP reconstruction and to correlate the MPI scan findings with the coronary angiography.

***Corresponding author:** Tore Bach-Gansmo, MD, PhD, Department of Radiology and Nuclear Medicine, Oslo University Hospital, Oslo, Norway, Tel: +47 93 268 963; Fax: +47 23 01 5554; E-mail: bat@uus.no

Received October 19, 2011; **Accepted** November 22, 2011; **Published** November 27, 2011

Citation: Naum A, Kleven-Madsen N, Biermann M, Johnsen B, Tvedt BA, et al. (2011) Quantitative Comparison of Myocardial Perfusion Defects using Different Reconstruction Algorithms. J Clinic Experiment Cardiol S5:002. doi:10.4172/2155-9880.S5-002

Materials and Methods

Study population

The characteristics of the study population are shown in Table 1. The study involved 20 patients (13 males, 8 females, median age 61 years, range 41–80 years) who underwent MPI followed by invasive coronary angiography (CAG) within 3 months, for any positive or equivocal findings for CAD at MPI (using OSEM 3D reconstruction algorithm). All patients underwent one-day, low-dose rest, high-dose stress Tc-99m Tetrofosmin myocardial perfusion SPECT. SPECT images were acquired between 15 and 30 minutes after rest injection and between 45 and 60 min after stress injection. All subjects were given 0.14 mg/kg/min dipyridamole intravenously over 4 min. Three minutes after the end of dipyridamole infusion, the radiopharmaceutical was injected through an antecubital vein. Hemodynamic data and 12-lead ECGs were recorded every minute during dipyridamole infusion. Informed consent was obtained from all patients after they received a detailed explanation of the procedure.

Spect/ct imaging protocol

All studies were completed with a 90°-angled dual-head integrated Symbia T6 SPECT/ CT camera equipped with low-energy, high-resolution collimators. Patients were placed in the supine position with arms up, and an end expiration CT scan was acquired before SPECT images using a tube current of 130 kV, effective mAs of 13, delay 3s, for an axial field of view covering the thorax from the lung apex to 1-2 cm below the diaphragm. Emission data were acquired with a matrix of 64x64 pixels and a 20% energy window centered at 140 keV. Further acquisition parameters were 32 projections, 180° orbit, and 25 s per projection. On a dedicated workstation (Syngo MMWP, Siemens Medical Solutions) images were reconstructed iteratively (10 iterations, 8 subsets, Gaussian filter, FWHM= 9.6) by using the OSEM 3D approach (e.soft "Flash3D," Siemens Medical Solutions) with compensation for collimator-detector response as described previously elsewhere [12,13]. Datasets were visually assessed for misregistration with a fusion/registration software tool (Syngo Advanced Fusion, Siemens Medical Solutions), and when needed, a manual realignment between SPECT and CT images was performed to improve the CT attenuation correction process (Figure 1). The raw data were again reconstructed using the FBP method (Butterworth filter, Order 5, with a cut off frequency of 0.45 cycles/cm) at the same reorientation and reslicing angles as was used by Flash 3D. The numbers of iterations and subsets as well as the post smoothing parameters used were those recommended by the software supplier for the acquisition type. (Siemens/4D-MSPECT, INVIA, Ann Arbor, MI).

Patient characteristic	Number of patients (%)
Abnormal rest ECG results	13 (65%)
Prior myocardial infarction	7 (35%)
Prior catheterization	7 (35%)
Revascularization PTCA CABG	 5 (25%) 2 (10%)
Pacemaker	2 (10%)
Hypertension	9 (45%)
Diabetes	2 (10%)

CABG= coronary artery bypass graft; ECG= electrocardiogram; PTCA= percutaneous transluminal coronary angioplasty

Table 1: Characteristics of the study population.

	Variable		Abn. segm (N)	Mean	SD	SEM	95% CI of Mean
Extent %	*Flash 3D*						
		LAD	17	31.94	23.58	5.71	19.81 to 44.06
		LCx	17	29.52	23.65	5.73	17.36 to 41.68
		RCA	17	41.88	27.70	6.71	27.63 to 56.12
	FBP						
		LAD	12	25.08	22.44	6.47	10.82 to 39.34
		LCx	13	25.61	23.90	6.62	11.17 to 40.06
		RCA	9	25.00	23.74	7.91	6.74 to 43.25
Stress Severity Score	*Flash 3D*						
		LAD	17	3.77	0.89	0.24	3.23 to 4.31
		LCx	17	3.80	1.11	0.29	3.15 to 4.44
		RCA	17	3.75	0.56	0.15	3.43 to 4.08
	FBP						
		LAD	12	3.49	1.19	0.31	2.80 to 4.18
		LCx	13	3.73	1.36	0.39	2.86 to 4.60
		RCA	9	3.52	0.92	0.30	2.80 to 4.23
Extent %	*Flash 3D*						
		LAD	19	27.47	21.78	4.99	16.97 to 37.97
		LCx	18	22.77	17.57	4.14	14.03 to 31.51
		RCA	19	26.84	21.91	5.02	16.27 to 37.40
	FBP						
		LAD	11	26.54	22.29	6.72	11.56 to 41.52
		LCx	14	19.21	18.71	5.02	8.40 to 30.02
		RCA	11	24.09	19.36	5.83	11.07 to 37.10
Rest Severity score	*Flash 3D*						
		LAD	19	3.39	1.29	0.33	2.67 to 4.10
		LCx	18	3.33	1.34	0.34	2.59 to 4.07
		RCA	19	3.75	0.56	0.15	3.43 to 4.08
	FBP						
		LAD	11	3.56	1.11	0.32	2.85 to 4.27
		LCx	14	3.46	1.08	0.29	2.83 to 4.09
		RCA	11	3.52	0.92	0.30	2.80 to 4.23

Abn. Segm (N) – number of affected segments (in a bull-eye representation). CI - confidence interval; FBP - filtered back projection; Flash 3D-Siemens proprietary 3D iterative reconstruction algorithm; SD - standard deviation; SEM - standard error of the mean.

Table 2: Comparative description of FBP and Flash 3D derived defect extent (number of segments and in %) and severity.

	Flash 3D				FBP			
	Overall	LAD	LCx	RCA	Overall	LAD	LCx	RCA
TP n(%)	15 (75)	8 (40)	6 (30)	10 (50)	14 (70)	8 (40)	5(25)	6 (30)
FP n(%)	4 (20)	9 (45)	9 (45)	5(25)	4 (20)	4 (20)	8 (40)	3 (15)
TN n(%)	1 (5)	2 (10)	4 (20)	4 (20)	1 (5)	7 (35)	6 (30)	6 (30)
FN n(%)	0	1(5)	1(5)	1(5)	1 (5)	1(5)	1(5)	5(25)

FBP - filtered back projection; Flash 3D-Siemens proprietary 3D iterative reconstruction algorithm; FN - false negative; FP - false positive; TN - true negative; TP - true positive

Table 3: Assessment of MPI interpretation using Flash 3D and FBP against coronary angiography as the standard of reference.

Data analyses

Polar map plots were generated for both stress and rest cardiac tomograms. Normal databases matching the criteria of the selected dataset (gender specific, image acquisition performed in the same physiologic state, specific image based reconstruction technique) were used to define normal myocardial perfusion. Myocardial perfusion defects were automatically identified as areas with counts below the lower limit of normal (2.5 SD's as compared with the corresponding database). The extent of the perfusion defect was expressed as a percentage of the left ventricular surface area and the severity, as units of standard deviations (SD) below the normal mean. In addition, the correlation between the anatomic localization of the stenotic lesions and the location of detected perfusion defects were assessed using the polar map displays and a coronary artery distribution model template

included in the software package (Siemens/4D-MSPECT, INVIA, Ann Arbor, MI).

The image quality of FBP and Flash 3D reconstruction was characterized using three quantitative criteria: contrast (C), contrast to noise ratio (CNR) and signal to noise ratio (SNR). Contrast (C) was calculated between two regions of interest (ROIs) drawn inside the LV wall and cavity. The mean numbers of counts in these two ROIs were calculated, and the contrast was defined as:

$$C = \frac{A_{Myo} - A_{Cavity}}{A_{Myo} + A_{Cavity}} \times 100$$, where A_{Myo} and A_{Cavity} are the mean number of counts of the LV wall and the LV cavity, respectively

Noise (σ_{Myo}) was estimated as the standard deviation of the mean number of counts of the myocardial ROI.

Contrast to noise ratio (CNR) was determined as the ratio between contrast over the noise:

$$CNR = \frac{C}{\sigma Myo}$$

SNR in the myocardium region was calculated as the ratio between the mean number of counts over the noise:

$$SNR = \frac{A_{Myo}}{\sigma_{Myo}}$$

Statistical analyses

Data from the 2 reconstruction methods were compared using the paired t test. Independent groups were compared using an independent t test or 1-way ANOVA with Bonferonni correction. The Fisher exact test was used for comparison of proportional data. The estimates of left ventricle perfusion defects (percentage of left ventricular defect and severity scores) between the two reconstruction methods were compared using the Bland-Altman method of comparison [14] and Pearson correlation coefficient. A P value of less than 0.05 was considered statistically significant. All statistical tests were performed with MedCalc for Windows (MedCalc Software, Mariakerke, Belgium).

Results

Coronary angiography

The coronary arteries have been found to be normal on invasive coronoary angiography in five of the 20 patients (25%). A significant stenosis (arterial narrowing exceeding 50% of the lumen diameter) was present in the left anterior descending coronary artery (LAD) in 9 cases, left circumflex artery (LCx) in 6 cases and right coronary artery (RCA) in 11 cases. Single vessel disease was present in six patients (30%), double vessel disease in 7 (35%) and triple vessel in 2 (10%) patients.

Characterization of myocardial perfusion defects

The corresponding polar maps of myocardial perfusion were assigned to one of the three major coronary arteries using a standard template. All myocardial perfusion defects were automatically quantified for the extent and severity with both SPECT reconstruction methods (Figure 2). Descriptive statistics for the perfusion defect measurements are shown in Table 2 and Figure 3.

Perfusion defects on stress images: A total of 60 myocardial segments were included in stress analysis: 51 (85%) showed decreased perfusion with Flash 3D and 34 (57%) with FBP reconstruction. The mean differences in defect extent between the two methods of reconstruction were 6% for the LAD artery, 4% for the LCx and 17% for the RCA artery. Correspondingly, the mean differences in severity scores were 0.3SD's for the LAD, 0.1SD's for the LCx and 0.2 SD's for the RCA. No significant differences were found between the two methods of reconstruction regarding the defect extent and severity during stress. When all defect extent and severity scores of all coronary arteries were pooled, the Bland-Altman method of comparison revealed an observed bias of -15 ± 20.73% (overall correlation coefficient, r=0.63) for the

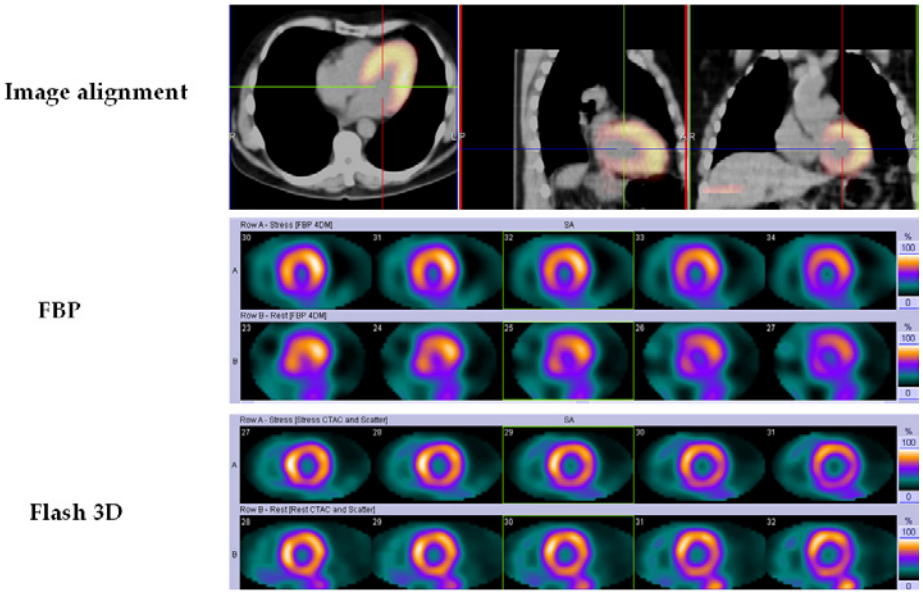

Figure 1: The resulting image from FBP and Flash 3D reconstruction. Top row shows the alignment of cardiac data matching CT and SPECT images. Middle row shows midventricular short-axis slices reconstructed with FBP. Note the presence of an inferior wall perfusion defect on stress-rest images indicating an inferior wall myocardial infarction. Bottom row shows midventricular short axis slices reconstructed with Flash 3D. Note the absence of the inferior wall defect, suggesting that this was an artifact. Also, better contrast between the left ventricular walls and cavity and better visualization of the right ventricle.

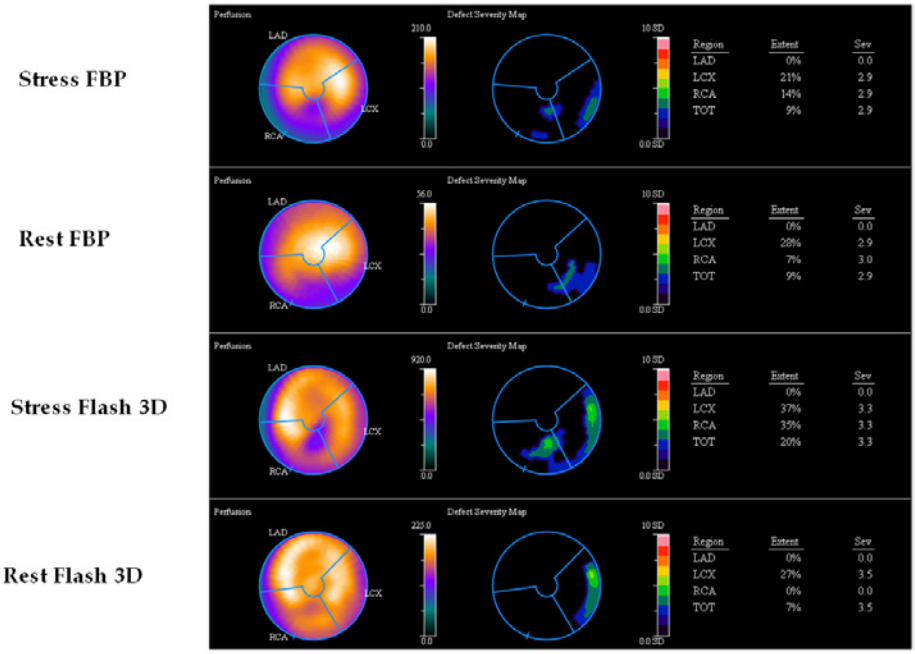

Figure 2: The coronary artery territory template used for defect extent and severity scores quantification with both reconstruction methods.

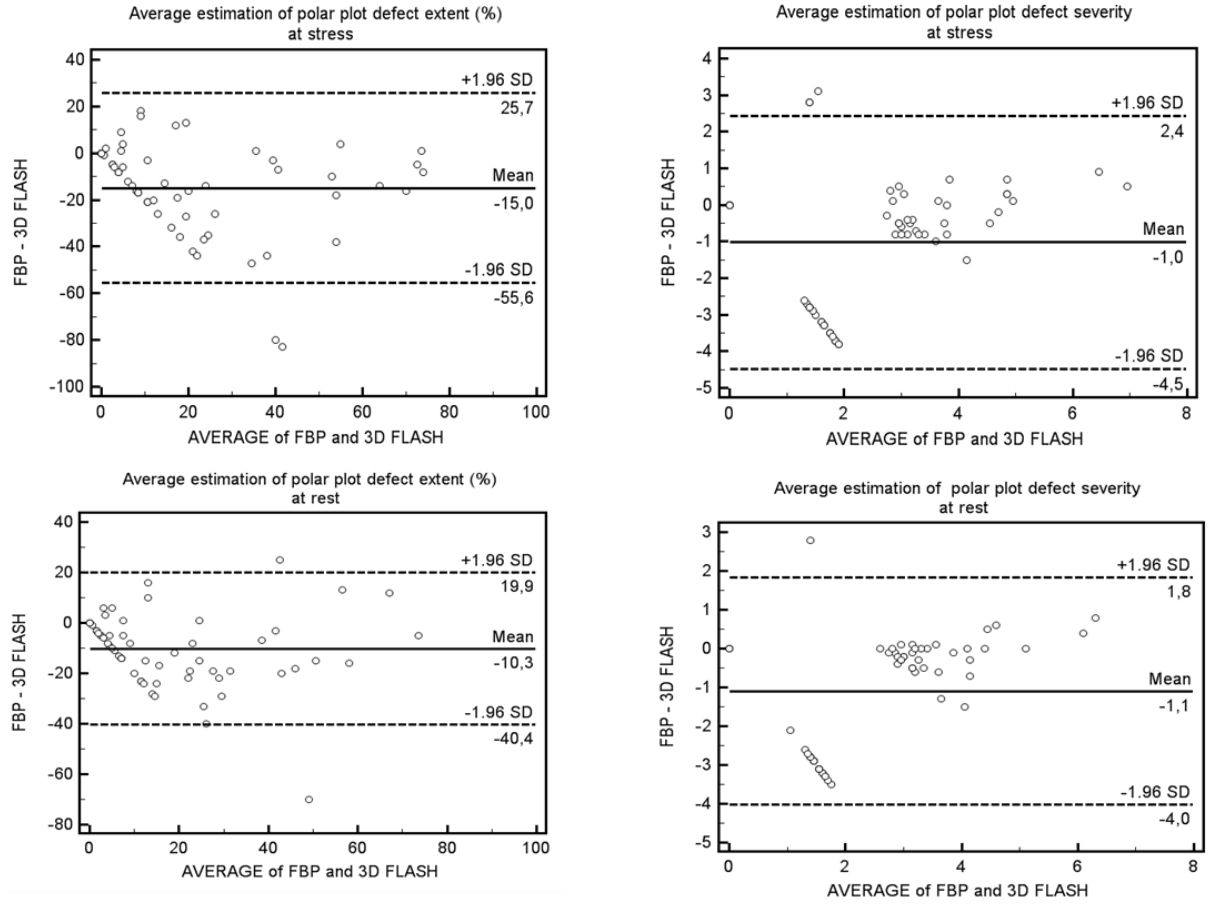

Figure 3: Comparison of the defect extent results (left side) and severity scores (right side) at stress (upper row) and rest (bottom row) obtained with FBP and Flash 3D reconstruction techniques according to the Bland-Altman graphic method.

defect extent measurement, and a bias of -1.02±1.77 SD's (overall correlation coefficient, r=0.62) for the severity score.

Perfusion defects on rest images: Of 60 myocardial segments studied, decreased myocardial perfusion was found in 56 (93%) in Flash 3D based reconstructions and in 36 (60%) in FBP. The mean differences in defect extent between the reconstruction methods were 1%, 4% and 3% within the vascular territory of LAD, LCx, and RCA, respectively. Mean severity scores slightly increase in FBP by 0.2 SD's within the LAD and by 0.1 SD's in LCx and decrease by 0.2 SD's within the RCA vascular territories. No significant differences were encountered between the two methods of reconstruction at rest. Bland-Altman analysis for pooled data showed a bias of -10.27±15.37% (overall correlation coefficient, r=0.70) for the defect extent size, and a bias of -1.10±1.49 SD's (overall correlation coefficient, r=0.61) for severity scores.

Comparison between coronary angiography and SPECT-MPI

All MPI studies exhibiting stress perfusion defects were considered abnormal. The overall level of disagreement (number of false-negative and false-positive cases) for CAD detection against coronary angiography results was comparable in Flash 3D and in FBP image-based reconstructions, (4 cases vs.5 cases, P=NS). The distribution of true positive (TP), false positive (FP), true negative (TN), or false negative (FN) perfusion defects according to the reconstruction technique and anatomic localization of the stenotic lesions is shown in Table 3. The disagreements for the absence or presence of perfusion defects in the coronary artery territories using Flash 3D were slightly higher in the LAD and lower in the RCA coronary territory as compared to the FBP, but no statistical significance was reached.

Image quality evaluation

Flash 3D reconstruction algorithm significantly increases the image contrast by 31% (P=0.002) during stress (from 30 to 61%, P=0.005) and at rest (from 11 to 42%, P< 0.001). A trend towards a decrease in SNR and CNR values was found during stress (from 9.04±3.34 to 7.64±2.68 for SNR, P=NS and from 0.52±0.84 to 0.22±0.11 for CNR, P=NS) and at rest (from 9.34±2.93 to 8.56±3.23 for SNR, P=NS and from 0.71±1.49 to 0.63±0.36 for CNR, P=NS) as compared with FBP.

Discussion

The present study was performed to assess the feasibility of an OSEM reconstruction algorithm and CT- based attenuation correction (Flash 3D), which has been reported to improve image quality and quantitation performance by applying compensation techniques for photon attenuation, Compton scatter and 3-dimensional depth-dependent resolution [12,13,15]. First, we compared the impact of Flash 3D versus FBP on myocardial perfusion defect and severity quantification in 20 patients who had undergone both stress-rest myocardial perfusion SPECT and coronary angiography. Our results indicated that there was no statistically significant difference in myocardial perfusion defect extent and severity using Flash 3D versus FBP. This study showed that the number of patient images with perfusion defects was identical with Flash 3D and FBP reconstruction. Small differences in perfusion defect extent (up to 6%) were encountered in individual coronary artery territories with Flash 3D against FBP, except the RCA vascular territory (17% mean difference during stress), but no statistical significance was reached. The difference in mean severity scores was negligible, with the highest value of 0.3 SD's found in the LAD coronary territory during stress. With respect to individual vascular territories (Table 3), the disagreements between the two types of reconstruction were mostly in the RCA and LCx arteries. This is probably due to the effect of subdiaphragmatic activity and diaphragmatic attenuation especially in the case of inferior wall which is not corrected in FBP reconstruction. This finding may suggest that, although the compensation techniques for the photon attenuation and scatter might be effective with Flash 3D, it does not decrease the difficulties associated with the inferior wall attenuation artifacts [16]. Also, a certain degree of misregistration might be present between SPECT and CT data, even after manual realignment. Scatter as well, may contribute, since all patients underwent pharmacologic stress with dipyridamole, well-known for the high radiopharmaceutical uptake in the liver [17]. Nevertheless, the use of a standard template of coronary arteries distribution in MPI perfusion analysis may have also influenced. For instance, if a perfusion defect lies in the RCA territory, slightly increased perfusion defect size in Flash 3D reconstruction will incorporate part of the LCx territory as well [18]. Summarizing, Flash 3D algorithm provides results equivalent to conventional FBP in terms of quantitative myocardial perfusion defect analysis and location as confirmed by coronary angiography.

Like previous studies [19-21] our results indicate that combined scatter, attenuation and detector response correction led to an increase in image quality. The contrast between the myocardial wall and the left ventricular cavity increases by 31%. Without any corrections (FBP reconstruction), the CNR and SNR values were higher, with a trend toward decreased values in Flash 3D reconstructed images that is consistent with a slight increase in image noise. This could be related to the increased number of iterations and subsets used in our study (10 iterations, 8 subsets) which may have an additive effect on noise as it has been suggested by other researchers [22,23]. Anyhow, Flash 3D reconstructed images are improved quantitatively by increasing the absolute values of image contrasts, while CNR and SNR values remain approximately equal to those measured in the FBP reconstructed images.

The small number of subjects studied is a major limitation of the study and subsequent large scale clinical implementation of this novel image reconstruction algorithm requires a further larger patient study rigorously tested in standardized conditions.

Conclusions

OSEM 3D image reconstruction algorithm (Flash 3D) with attenuation, scatter, and spatial resolution compensation proved to be superior to conventional FBP in terms of image contrast, and equivalent to FBP for specific clinical findings, and in particular does not decrease the difficulties associated with the inferior wall attenuation artifacts.

Acknowledgements

The authors wish to thank the staff of the Centre for Nuclear Medicine/PET for their excellent contribution in imaging patients.

References

1. Vitola JV, Shaw LJ, Allam AH, Orellana P, Peix A, et al. (2009) Assessing the need for nuclear cardiology and other advanced cardiac imaging modalities in the developing world. J Nucl Cardiol 16: 956-961.

2. Hendel RC, Berman DS, Di Carli MF, Heidenreich PA, Henkin, RE et al. (2009) ACCF/ASNC/ACR/AHA/ASE/SCCT/SCMR/SNM 2009 appropriate use criteria for cardiac radionuclide imaging: a report of the American College of Cardiology Foundation Appropriate Use Criteria Task Force, the American Society of Nuclear Cardiology, the American College of Radiology, the American Heart Association, the American Society of Echocardiography, the Society of Cardiovascular Computed Tomography, the Society for Cardiovascular Magnetic Resonance, and the Society of Nuclear Medicine: endorsed by the American College of Emergency Physicians. Circulation 119: e561–e587.

3. Garcia EV, Faver TL (2009) Advances in nuclear cardiology instrumentation: clinical potential of SPECT and PET. Curr Cardiovasc Imaging Rep 2: 230–237.
4. Bruyant PP (2002) Analytic and iterative reconstruction algorithms in SPECT. J Nucl Med 43: 1343-1358.
5. Slomka PJ, Patton JA, Berman DS, Germano G (2009) Advances in technical aspects of myocardial perfusion SPECT imaging. J Nucl Cardiol 16: 255-276.
6. Garcia EV, Faber TL (2009) New trends in camera and software technology in nu clear cardiology. Cardiol Clin 27: 227-236.
7. Pazhenkottil AP, Ghadri JR, Nkoulou RN, Wolfrum M, Buechel RR, et al. (2011) Improved outcome prediction by SPECT myocardial perfusion imaging after CT attenuation correction. J Nucl Med 52: 196-200.
8. Madsen MT (2007) Recent advances in SPECT imaging. J Nucl Med 48: 661-673.
9. Wolak A, Slomka PJ, Fish MB, Lorenzo S, Berman DS, et al. (2008) Quantitative diagnostic performance of myocardial perfusion SPECT with attenuation correction in women. J Nucl Med 49: 915-922.
10. Valenta I, Treyer V, Husmann L, Gaemperli O, Schindler MJ, et al. (2010) New reconstruction algorithm allows shortened acquisition time for myocardial perfusion SPECT. Eur J Nucl Med Mol Imaging 37: 750-757.
11. Ficaro EP, Fessler JA, Shreve PD, Kritzman JN, Rose PA, et al. (1996) Simultaneous transmission/emission myocardial perfusion tomography. Diagnostic accuracy of attenuation-corrected 99mTc-sestamibi single-photon emission computed tomography. Circulation 93: 463-473.
12. Stansfield EC, Sheehy N, Zurakowski D, Vija AH, Fahey FH, et al. (2010) Pediatric 99mTc-MDP bone SPECT with ordered subset expectation maximization iterative reconstruction with isotropic 3D resolution recovery. Radiology 257: 793-801.
13. Zeintl J, Vija AH, Yahil A, Hornegger J, Kuwert T (2010) Quantitative accuracy of clinical 99mTc SPECT/CT using ordered-subset expectation maximization with 3-dimensional resolution recovery, attenuation, and scatter correction. J Nucl Med 51: 921-928.
14. Bland JM, Altman DG (1986) Statistical methods for assessing agreement between two methods of clinical measurement. Lancet 1: 307-310.
15. Hughes T, Shcherbinin S, Celler A (2009) A multi-center phantom study comparing image resolution from three state-of-the-art SPECT-CT systems. J Nucl Cardiol 16: 914-926.
16. Celler A, Shcherbinin S, Hughes T (2010) An investigation of potential sources of artifacts in SPECT-CT myocardial perfusion studies. J Nucl Cardiol 17: 232-246.
17. Pretorius PH, Narayanan MV, Dahlberg ST, Leppo JA, King MA (2001) The influence of attenuation and scatter compensation on the apparent distribution of Tc-99m sestamibi in cardiac slices. J Nucl Cardiol 8: 356-364.
18. Javadi MS, Lautamäki R, Merrill J, Voicu C, Epley W, et al. (2010) Definition of vascular territories on myocardial perfusion images by integration with true coronary anatomy: a hybrid PET/CT analysis. J Nucl Med 51: 198-203.
19. Hendel RC, Berman DS, Cullom SJ, Follansbee W, Heller GV, et al. (1999) Multicenter clinical trial to evaluate the efficacy of correction for photon attenuation and scatter in SPECT myocardial perfusion imaging. Circulation 99: 2742-2749.
20. El Fakhri G, Buvat I, Benali H, Todd-Pokropek A, Di Paola R (2000) Relative impact of scatter, collimator response, attenuation, and finite spatial resolution corrections in cardiac SPECT. J Nucl Med 41: 1400-1408.
21. Fricke E, Fricke H, Weise R, Kammeier A, Hagedorn R, et al. (2005) Attenuation correction of myocardial SPECT perfusion images with low-dose CT: evaluation of the method by comparison with perfusion PET. J Nucl Med 46: 736-744.
22. Yokoi T, Shinohara H, Onishi H (2002) Performance evaluation of OSEM reconstruction algorithm incorporating three-dimensional distance-dependent resolution compensation for brain SPECT: a simulation study. Ann Nucl Med 16: 11-18.
23. Brambilla M, Cannillo B, Dominietto M, Leva L, Secco C, et al. (2005) Characterization of ordered-subsets expectation maximization with 3D post-reconstruction Gauss filtering and comparison with filtered backprojection in 99mTc SPECT. Ann Nucl Med 19: 75-82.

This article was originally published in a special issue, **Myocardial Infarction and Protection** handled by Editor(s). Dr. Dayue Darrel Duan, University of Nevada, USA